

Investigating the Impact of Communication Errors on the Transient Characteristics of Power Systems

Ahmed Abdolkhalig

Department of Electrical Engineering, The University of Tobruk, 4004, Tobruk, Libya

Received December 9, 2022; Revised March 22, 2023; Accepted April 16, 2023

Cite This Paper in the Following Citation Styles

(a): [1] Ahmed Abdolkhalig , "Investigating the Impact of Communication Errors on the Transient Characteristics of Power Systems," *Universal Journal of Electrical and Electronic Engineering*, Vol. 10, No. 2, pp. 13 - 28, 2023. DOI: 10.13189/ujeee.2023.100201.

(b): Ahmed Abdolkhalig (2023). *Investigating the Impact of Communication Errors on the Transient Characteristics of Power Systems*. *Universal Journal of Electrical and Electronic Engineering*, 10(2), 13 - 28. DOI: 10.13189/ujeee.2023.100201.

Copyright©2023 by authors, all rights reserved. Authors agree that this article remains permanently open access under the terms of the Creative Commons Attribution-NonCommercial 4.0 International License

Abstract As communication errors change in the dynamic properties of the protection relay and control system, the preset relay tripping time is no longer applicable. To ensure reliable operations and avoid any problem linked to grid stability, the impact of these errors on the transient characteristics of the power system must be investigated. To investigate the impact, a very simple and effective scheme based on an Ethernet communication network is proposed in this paper. The scheme relies on Inverse definite minimum time (IDMT) digital over-current relay which has two added functions, one is for phasor estimation and the other is for detecting the delays in tripping time. First, the IDMT over-current relay is fed by fundamental amplitude from the phasor estimator through an Ethernet-based network. Next, the delay that arises due to the insufficient allocation of bandwidth or noise is detected and measured by the detection function. Finally, to evaluate the impact of the communication errors on tripping time and consequently, on the transient characteristics of the power system, a test system consisting of a plant and two sources is simulated and analyzed using MATLAB software in combination with True-Time software. The results show that impact of these errors is dramatic and cannot be ignored especially when insufficient bandwidth is allocated.

Keywords Digital Relay, Fault Clearing Time, Phasor Estimation, Transient Stability

1. Introduction

The occurrence of faults in electric power transmission networks can cause transient in both medium and high voltage networks. This transient is typically a three-phase positive sequence signal which tends to diverge both of generator rotor speed and voltage phase angle. The amplitude of voltage does not have a growing tendency except for the cases of shedding large loads or leading power factor tripping. Protective relay systems should be able to distinguish between a dynamic, but stable power swing and an actual fault.

To prevent any undesirable tripping signals during short circuits or transient phenomena, under-voltage protection relays are often configured so they have a long-time delay (typically, in seconds). This may put the relays exposed to the risk of malfunction due to its inability to detect the delays in relay tripping time linked to communication errors. Therefore, such protective schemes are ineffective and it is of vital importance to find an accurate detection scheme for tripping delays to maintain the stability and operational reliability of the power system.

Since the advent of the first commercial digital relay that was introduced in 1980 and more recently, the Ethernet-based communication digital relays, they have played a key role in the protection and operation of power systems [1, 2]. Digital protection relay (DPR) is typically installed in the electric power substation switching yard (switchyard) to continuously monitor, detect and isolate any possible system fault and disturbance (e.g., power swing).

The operational reliability of DPR is depending on the accuracy of the estimation for amplitude and phase angle of the measured signals (i.e., voltage or current) that is received from measuring devices through the communication network. More precisely, it depends on the numerical algorithm for the estimation and the traffic performance of the communication network being used. These two factors are considered the main key factors that may affect the operation of the DPRs thus, their influence needs to be evaluated to ensure a reliable operation.

For the first key factor, most recent DPRs are widely designed and implemented based on the so-called Discrete Fourier Transform (DFT) algorithm. One of the shortages of adopting DFT-Based algorithm relay is that the estimation of the fundamental phasors is extremely destroyed when the measured signal is corrupted with noise [3-7]. Also, estimating an accurate fundamental phasor requires a full-cycle of samples to be used [8, 9]. If harmonics and inter-harmonics as defined in IEC 61000-2-1 standard [10] are presented in the signal, the accuracy will more decrease due to the effect of the leakage [11-14].

Many research works are being conducted in recent years in order to find a compact and reliable digital protection scheme. The proposed scheme presented in [15] is a digital over-current relay (OCR) based on estimating the peak value of the actual current by measuring the slope at the zero-crossing. The authors suggested three identical DPR units be used in this scheme to protect the three phases (each phase has a dedicated installed DPR unit). This work had not considered the noise that can deeply affect the accuracy when measuring zero crossing. Moreover; from an economic perspective, using three units may increase the production cost and eventually, will make this protection scheme not a good choice for many contractors. In another work, an estimation algorithm that was implemented based on the components of the DC off-set, the fundamental angular frequency, and the fundamental component of the fault signal is proposed in [16]. In this work, only the measurement noise effect is investigated. Research work in [17], proposed only an approach for the estimation of the parameters of a synchronous generator from the records of DPRs and, it not had considered the algorithm being adopted for estimating these records.

Some other recent research works proposed new digital protection schemes based on Kalman filtering algorithm (KF) whereas it was added as a built-in function in the DPR's structure for estimating the fundamental phasor. Those proposed schemes are mainly depended on traditional algorithms of KF such as the Linear Kalman filter (LKF) or the non-linear version of the extended Kalman filter (EKF) [18-22]. Power systems are mainly characterized by highly non-linear dynamics and therefore, a high accuracy of estimation may not be achieved even with the EKF-based protection schemes. A novel development of traditional EKF which is defined as the

Unscented Kalman Filter (UKF) can combine between better linearization of a highly non-linear system, noise filtering and the high performance in real-time applications. More details about UKF algorithm will be given next section.

In recent years, there are some applications of UKF algorithm for estimating the fundamental phasor in conjunction with digital relays. The schemes proposed in [17, 23, 24] are schemes relied on the estimation of dynamic states and parameters of a synchronous generator by UKF from DPR records which already implemented based on DFT. Also, the scheme proposed in [16] is just a MM-UKF algorithm for digital relay protection. The algorithm constructed is just to estimate the fundamental component, whereas the estimation is done by utilizing multi-scale decomposition signals that are previously obtained from morphological filter. This multi-scale decomposition can lead to increase the computation burden.

For the second key factor, most power utilities in recent years have started adopting deterministic real-time Ethernet-based communications networks for data transfer. One of the main obstacles in the way of adopting such communication networks is the determinism (i.e., time span) in which a response is expected to be unpredictable. Correct allocation of bandwidth (BW) can be considered the main factor that can improve determinism. One of the earliest research works that was considered the issue of determinism and how it can be affected by the insufficient allocation of BW is presented in [25]. The authors in this work presented the characteristics that are required from the algorithm of the digital relay so it can tackle the streams of data arriving through the data packets.

More recently, the authors in [26] proposed a line current differential protection scheme over IP-based networks. The use of IP-based networks does not assure data transmission in real-time, because of retrieving the data through a series of requests and responses. In [27], authors are just defined how a new source of asymmetry may arise due to the use of de-jitter, which can put the Ethernet network-based protection scheme at higher risk. The authors also did not consider the risk that may arise due to the allocation of BW that is insufficient. Allocating inappropriate BW can minimize the operational reliability, speed, and sensitivity of protection scheme and therefore, the relay performance needs to be evaluated against network BW allocation.

Based on this literature review, there is a necessity for finding a scheme that is solely able to accurately track the fundamental component and to detect any delay in the relay tripping time in real-time.

This paper is a continuation of the work presented in [28] and it provides more contributions as it adds more functions to the protection scheme as it can detect the delay in relay tripping time that may arise due to the communication network errors. The detection of delay is accomplished by a built-in function in the scheme which

works side-by-side with UKF function based on measurements being received via the real-time network.

Furthermore, the paper provides a detailed evaluation of misallocation of BW and noise impact on the relay tripping time and consequently, how this impact can influence the transient characteristics of power system. The paper evaluates the impacts of misallocation of BW and noise for media access control (MAC) types that are most used to establish Ethernet-based networks.

The remainder of the paper is organized as follows: section-2 explains the methodology of the design and the implementation of the proposed protection scheme. It starts with giving an introductory part to the Kalman filtering algorithm and then, explains the newly developed functions for the estimation of the amplitude and the detection of the time delay, respectively. Section-3 gives details about the test system being used. It also presents the results of evaluating the network errors and how they can affect the performance of the DPR and consequently, the transient stability. More results are also given for evaluating the noise effect on power stability. Section-4 gives conclusions and future work.

2. Methodology

The proposed scheme is depicted in the schematic diagram of Figure 1. As it shown in the diagram, the scheme has two added functions; the first function is to estimate the phasor, and the purpose of the other function is to detect the delay in the tripping time. The DPR is implemented as an inverse definite minimum time (IDMT)

over-current relay (OCR) as defined in the IEC60255 standard [29] for electric relays. According to this standard, the mathematical description of standard *SI* inverse time-current characteristic of an over-current relay can be written as in Eq. (1) below:

$$T = TMS \times \frac{K}{I_a^n - 1} \quad (1)$$

where, I_a is the normalized fault current (i.e., $I_a = \frac{I_c}{I_p}$); I_c and I_p are the actual and pickup current, respectively. 'K' is a constant which represents the relay operating time, 'n' represents the relay inverse characteristics and *TMS* is the time multiplier setting. Figure 2 depicts the schematic diagram of the implemented OCR. In this schematic diagram, it is required that the relay operates or picks up when its current exceeds a pre-determined value (setting value). Also in this schematic diagram, it is required that the fundamental amplitude of the actual measured value (I_c) is raised to a power of n and then integrated as follows in Eq. (2):

$$\text{Intg} = \int I_c^n dt \quad (2)$$

To get the amplitude of I_c , the actual measured value that is a dynamic three-phase current signal corrupted with noise should be converted to one stationary reference signal and noise filtered out. This will be done by employing the UKF algorithm. The next sub-sections explain how to implement the UKF and time delay detection functions, respectively.

Implementation of phasor estimator function

It is mentioned in section-1 that, those protection schemes designed and implemented based on the DFT algorithm or traditional algorithms of KF have many drawbacks. The extreme distortion of estimate when the measured signal is corrupted with noise and the poor representation of the high non-linearity functions can be considered the main drawback of DFT algorithm and traditional algorithms of KF, respectively.

Compared to DFT and KF algorithms, UKF is an algorithm that most accurately estimates variables of highly non-linear and noisy systems [30-34]. Also, UKF can be more advantageous in real-time applications due to the use of a deterministic sampling technique known as the unscented transform. This transform picks a minimal set of sample points (so-called sigma points) and propagates them through the non-linear system. The algorithm starts by transforming the non-linear system equations to recursive non-linear system discrete equations as follows in Eq. (3) and (4):

$$\mathbf{x}_{k+1} = \Phi_k \mathbf{x}_k + \mathbf{w}_k \quad (3)$$

$$\mathbf{z}_k = \mathbf{H}_k \mathbf{x}_k + \mathbf{v}_k \quad (4)$$

where \mathbf{x}_k is the discrete state vector, \mathbf{z}_k is the discrete measurements vector; Φ_k is the state transition matrix; \mathbf{H}_k is the discrete measurement matrix; \mathbf{w}_k is the discrete driving noise and \mathbf{v}_k is the discrete measurement noise.

If the discrete state vector has a dimension of $N \times 1$, then; there are $2N$ sigma points $\mathbf{x}_k^{(i)}$ with mean $\bar{\mathbf{x}}_k$ and covariance \mathbf{P}_{xx} . The sigma points around the states can be calculated from Eq. (5), Eq. (6) and Eq. (7) below.

$$\mathbf{x}_k^{(i)} = \bar{\mathbf{x}}_k + \tilde{\mathbf{x}}_k^{(i)}, \quad i = 1, \dots; 2N \quad (5)$$

$$\tilde{\mathbf{x}}_k^{(i)} = (\sqrt{N\mathbf{P}_{xx}})^t, \quad i = 1, \dots; N \quad (6)$$

$$\tilde{\mathbf{x}}_k^{(N+i)} = -(\sqrt{N\mathbf{P}_{xx}})^t, \quad i = 1, \dots; N \quad (7)$$

The sigma points can be related to these state variables as in Eq. (8).

$$\mathbf{X}_k = [\bar{\mathbf{x}}_k, \bar{\mathbf{x}}_k \mp \sqrt{N\mathbf{P}_{xx}}] \quad (8)$$

Those sigma points can be propagated through the equation of measurement as $\mathbf{U}_k = h(\mathbf{X}_k)$ and eventually, the steps of the standard Kalman filtering algorithm process can be followed to get an accurate estimate of the state (i.e., the fundamental phasor). In this paper, the objective of the UKF Function implementation is to estimate the phasor of the fundamental component (positive-sequence) of the dynamic three-phase current signal.

Figure 3 shows the Schematic diagram of UKF function implementation. The phasor is firstly digitized at a standardized sampling rate and then synchronized to a reference time. The accuracy of the estimation function is

depending on the sampling rate that can be adopted. According to [35], the sampling frequencies of measured values are standardized at two frequency rates: SMV#1 that has 80 samples/cycle and SMV#2 that has 256 samples/cycle. SMV#1 is typically used for power control and protection applications whereas SMV#2 is used for power quality studies and applications. In this paper, SMV#1 (4 kHz) rate is adopted.

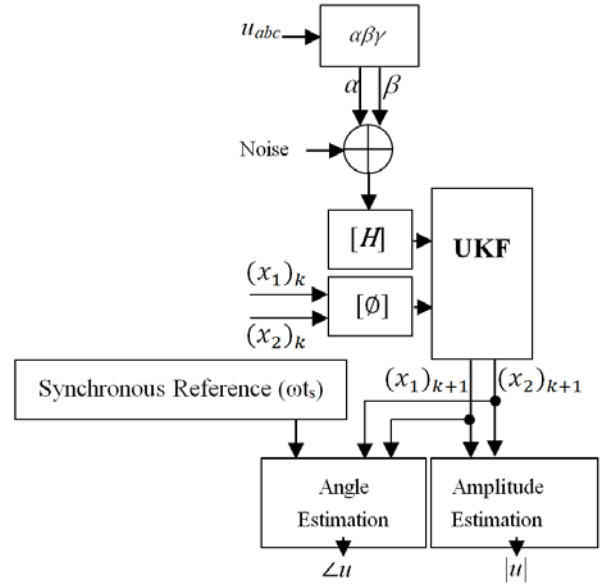


Figure 3. Schematic diagram of UKF function implementation.

The amplitude of the estimated fundamental phasor represents the peak actual value (I_c) which can be used to feed the DPR. To get an estimate of the amplitude, the three-phase current signals of I_c are collapsed to one stationary reference frame as follows in Eq. (9):

$$\begin{bmatrix} (I_{c\alpha})_k \\ (I_{c\beta})_k \end{bmatrix} = \mathbf{T} \cdot \begin{bmatrix} (I_{ca})_k \\ (I_{cb})_k \\ (I_{cc})_k \end{bmatrix} + (r_{\alpha\beta})_k \quad (9)$$

where \mathbf{T} is the Clark Transformation ($\alpha\beta\gamma$ Transformation) [36]. And in a complex form, Eq. (9) can be expressed as in Eq. (10):

$$(I_{c\alpha\beta})_k = (I_{c\alpha})_k + j(I_{c\beta})_k \quad (10)$$

where,

$$(I_{c\alpha})_k = A_k \cdot \cos(\omega\Delta t + \varphi_k) \quad (11)$$

$$(I_{c\beta})_k = A_k \cdot \sin(\omega\Delta t + \varphi_k) \quad (12)$$

Assume that $(I_{c\alpha})_k = (x_1)_k$ and $(I_{c\beta})_k = (x_2)_k$ and from trigonometric identities, Eq. (11) and (12) can be rewritten as in Eq. (13) and Eq. (14).

$$(x_1)_{k+1} = (x_1)_k \cdot \cos(\omega\Delta t) \dots - (x_2)_k \cdot \sin(\omega\Delta t) \quad (13)$$

$$(x_2)_{k+1} = (x_2)_k \cdot \sin(\omega\Delta t) \dots + (x_1)_k \cdot \cos(\omega\Delta t) \quad (14)$$

Eq. (13) and (14) can be expressed in matrix form as follows in Eq. (15).

$$\begin{bmatrix} (x_1)_{k+1} \\ (x_2)_{k+1} \end{bmatrix} = \Phi_k \begin{bmatrix} (x_1)_k \\ (x_2)_k \end{bmatrix}, \quad (15)$$

where $\Phi_k = \begin{bmatrix} \cos(\omega\Delta t) & -\sin(\omega\Delta t) \\ \sin(\omega\Delta t) & \cos(\omega\Delta t) \end{bmatrix}$ is representing the state transition matrix. Similarly, the measurement equations can be expressed in a matrix form as in Eq. (16):

$$(I_{c\alpha\beta})_k = [1 \quad j] \begin{bmatrix} (x_1)_k \\ (x_2)_k \end{bmatrix} \quad (16)$$

Thus, the estimated amplitude A_{k+1} of I_c can be calculated as $\sqrt{((x_1)_{k+1})^2 + ((x_2)_{k+1})^2}$. Hence, based on this value, the value of the integrator will keep rising until it equals to the pre-set value of constant K and at that moment; the relay will send its trip signal. Moreover, if the value of the excess current is temporary, the rising integral will be reset to zero.

Alternatively, if the DPR function is implemented based on a directional over-current relay then, an estimation of the directional angle is needed. The algorithm of UKF can sit to estimate the angle as follows in Eq. (17).

$$\hat{\phi}_{k+1} = \tan^{-1} \left(\frac{(x_2)_{k+1}}{(x_1)_{k+1}} \right) \quad (17)$$

Here, $\hat{\phi}$ is the estimated angle but not yet synchronized. To adjust the angle and make it synchronized, the following equation (Eq. 18) is applicable.

$$\delta_{k+1} = \frac{e^{-j(\hat{\phi}_{k+1} + \frac{\pi}{2})}}{e^{-j(2\pi f t_s)}} \times \frac{180}{\pi} \quad (18)$$

where f is the system nominal frequency and $\hat{\delta}$ is the estimated angle in degree. Here, t_s it represents the synchronous time reference, and it can be fed with a Global Positioning System (GPS) signal (In our simulation, the computer internal clock is used as a reference).

Implementation of delay detection function (DDF)

From basic studies of power stability, the requirement that should be satisfied in order to consider a power system is transiently stable is the maximum elapsed time from the initiation of the fault until its isolation should be less than the critical clearing time (t_{cr}) which can be calculated according to Eq. (19) below.

$$t_{cr} = \sqrt{\frac{4H(\delta_{cr} - \delta_0)}{\omega_s P_m}} \quad (19)$$

where, H is the inertia constant, δ_0 initially rotor angle ω_s is the synchronous speed and P_m is representing the shaft power input. In the schematic diagram of Figure 1, Kalman filtering function is implemented to estimate the fundamental value of I_c and transmit it to the digital relay over the communication network. According to the guideline [35], it is defined that the estimation of fundamental value and the transmission of it to the relay should be in real-time (In a period of time less than 3 milliseconds). This constraint imposed the use of fast and reliable communication networks such as Ethernet-based networks.

At present, Ethernet-based networks are established based on many media access control (MAC) models namely carrier sense multiple access with an arbitration on message priority CSMA/ AMP (e.g. CAN), carrier-sense multiple access with collision detection CSMA/CD (e.g. Ethernet), frequency division multiple access (FDMA), network control model (NCM), token bus (Round Robin), switched Ethernet, and time division multiple access (TDMA). Each one of these models has a different method to transmit data as follows: In CSMA/AMP model, when the network is busy, the sender node should wait until the network becomes free. When the collision occurs here, the message that has highest priority should be continued to be transmitted. If any two messages having same priority request a transmission at the same time, the priority can be decided by network in an arbitrary way to make which one is transmitted first.

In CSMA/CD model, the technique of transmission is same as the CSMA/AMP except that when there is a collision. In this case, this technique depends on the traffic collision avoidance. When the network is busy, the sender node will wait until the network becomes free. If there is any collision, the sender node will back off for a time defined by $t_{backoff} = (\text{minimum frame size}) / (\text{data rate} \times R)$ where $R = \text{rand}(0, 2K - 1)$ and K represents the number of collisions in one row. After the waiting time period, the node will reattempt to transmit the packet. In the FDMA model, the nodes have completely independent transmissions and thus, no collisions can occur. TDMA model is similar to the FDMA model except that a BW of 100% is allocated to each node in its scheduled slots. NCM is a model that allows the exchange of data with USB by setting up nodes to transmit IEEE 802.3 frames. Round Robin is another model that is similar to CSMA/AMP except that, the sender will idle for pre-defined back-off time between turns.

In switched Ethernet model, each sender node in the network has its full-duplex connection to the network central switch. In this manner, there are no any collisions on the network segments which provide best collision

avoidance compared to an ordinary Ethernet. The network central switch stores any received message in a buffer and then forwards it to the right destination receiving node. Despite the fact that those Ethernet-based communication networks have very small latency (delay) which makes this kind of communication network suitable for many protection applications, sample loss that occurs due to the insufficient of BW being allocated can affect the DPR's performance and thus, the impact of this latency needs to be evaluated.

As the aim of the work in this paper is to implement a very simple and effective function that can detect any delay in t_{trip} that may arise due to the network errors, the scheme should have a function that is solely able to detect such delay. Figure 4 represents the flow chart that is used to implement the delay detection function. The function works as follows: At any occurrence of fault, the fundamental value of actual current (I_c) will be compared with the pickup current (I_p). If $I_c > I_p$, the output of the integrator block will keep raising until it becomes equal to the pre-set value and thus, relay operates and sends a trip signal. The time at which the relay should operate is given as $t = K/I_c^n$ (operating time of the relay). The trip signal

being sent will pass through a zero-crossing detection block and the time records of t_{trip} are logged referenced to t_s (i.e., the reference time).

After that, the maximum value is taken to the logged values of time and then the delay can be calculated as $t_{delay} = t_{trip_max} - t$. Furthermore, the function will send a failure alarm/alert when the total opening time of CB (i.e., $t + t_{delay}$) is equivalent to or more than the critical clearing time. When there is alarm/alert, controllers should act rapidly to increase the BW allocation for protection node (DPR) so, the malfunction of the relay and thus instability of power systems can be avoided. The operational reliability of the DPR depends on the data being received which should be time-critical. If there is any time delay with the data being received, it may cause a failure or a maloperation. These time delay errors should be evaluated so that, a better relay setting can be recommended and thus, keep the limit of damage to a minimum level. The next section presents the simulation results of the impact BW allocation and noise on tripping time of relay (i.e., t_{delay}) and consequently, how they can affect the transient stability performance for a selected test system.

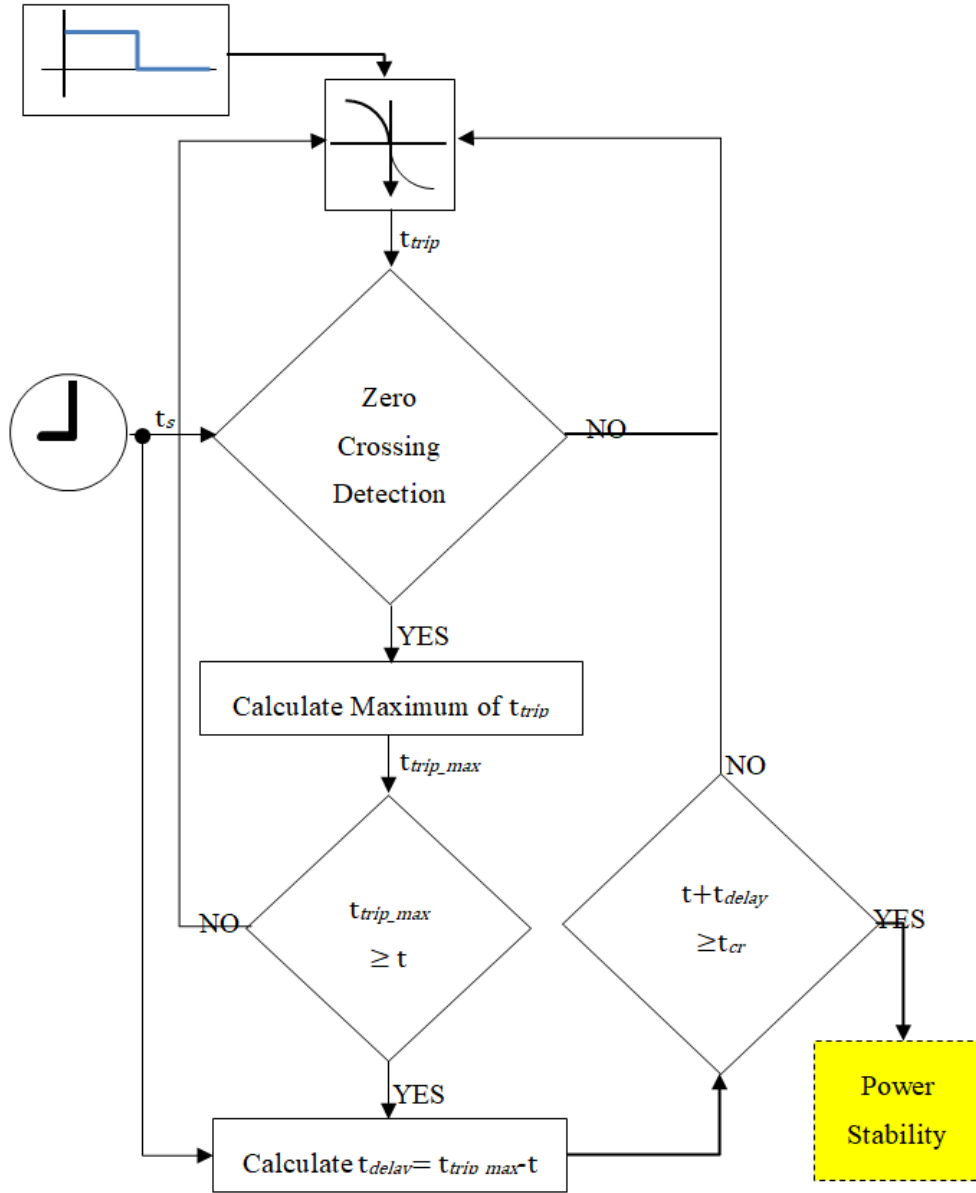


Figure 4. Flow chart of delay detection function.

3. Simulation Results

To evaluate the impact of time delay errors (that may arise due to the measurement noise or the insufficient allocation of BW) on the relay tripping time and consequently, on the transient stability of power systems; the three-machine system that is shown on the single line diagram of Figure 5 is used as a test system. It is simulated and analyzed using MATLAB software in combination with True-Time® software [37] for simulating the real-time communications.

The system consists of a plant (Busbar-2), simulated by a resistive load and motor load (ASM) fed at 2400 V from two sources: 1)- A distribution 25 kV network through a 6 MVA, 25/2.4 kV transformer, and 2)- An emergency synchronous generator/diesel engine unit (SM). A

capacitor bank of a 500 kVAR is used to correct the power factor at the 2.4 kV bus bar (Busbar-2). A simple R-L equivalent source (short-circuit quality factor of $X/R=10$ at level 1000 MVA) with a 5 MW load is used to model the 25 kV network. The ratings of the asynchronous motor and the synchronous machine are 2250 HP, 2.4 kV, and 3.125 MVA, 2.4 kV, respectively. At the start, the mechanical power developed by the motor is 2000 HP while the diesel generator is delivering an active power of 500 kW.

The voltage at busbar-2 is controlled by the synchronous machine which is kept constant at 1.0 pu. A fault of type three-phase to ground occurs on the 25 kV system at $t=0.5$ sec, causing a sudden increase of the generator loading and activating DPR to send a trip signal to the circuit breaker at 25 kV at a pre-set value of tripping time. The two current signals shown in Figure 6 are the fundamental

positive-sequence component of a dynamic three-phase current signal that the DPR is received and an estimated amplitude value of 78.5 A that the embedded estimation function is estimated before and after the occurrence of fault. When the fault occurs at $t = 0.5$ sec, the current value increases rapidly to ≈ 1400 A (i.e., ≈ 18 times more than nominal value) which should make the DPR react rapidly with a breaker opening time that is not more than 12 cycles (according to Eq. (19)). In our simulations, K and n are assigned values of 20 and 0.827, respectively so a fast-tripping time of 0.05 sec can be achieved for a fault current of 1400 A.

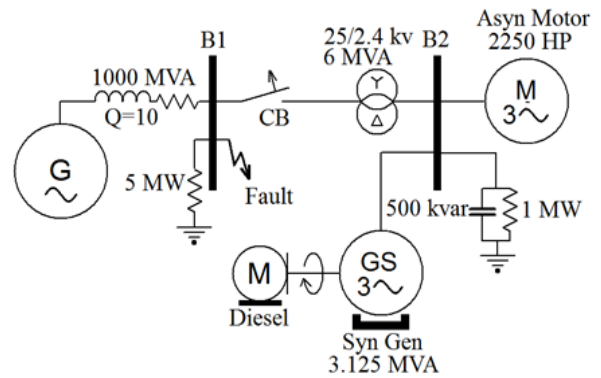


Figure 5. One-line diagram of the test system.

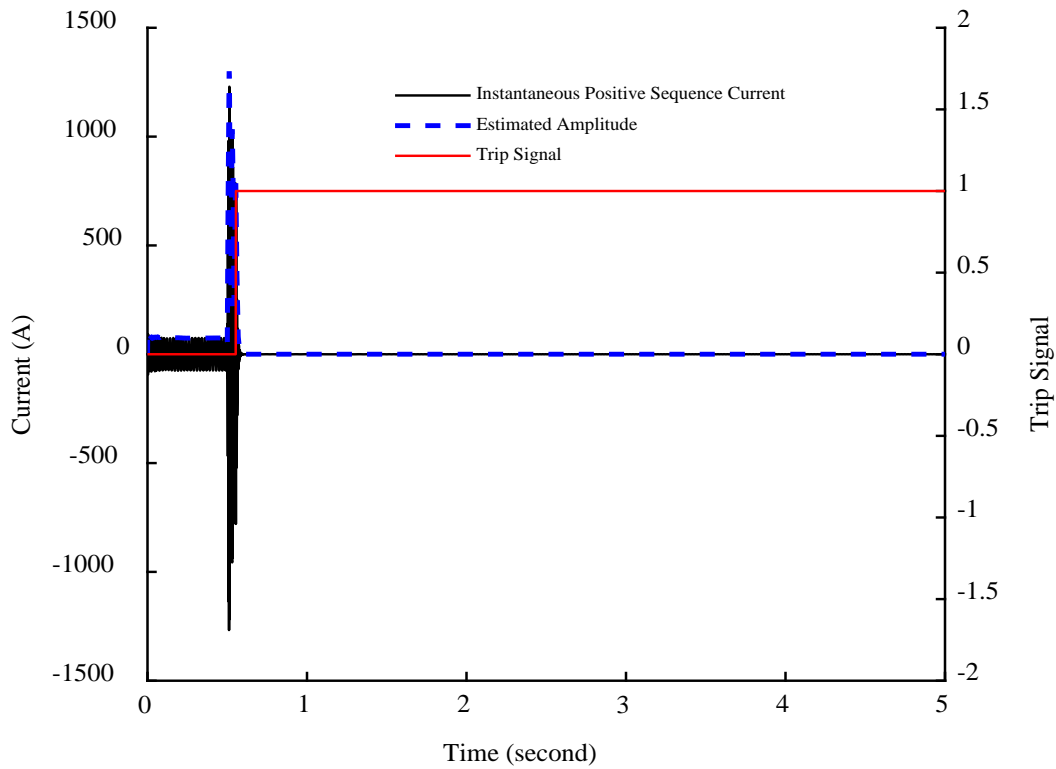


Figure 6. Current and trip signals performance.

After the fault detection, the integrator value will keep increasing until it equals to the pre-set value (i.e., $K=20$) and then, a trip signal will be sent by the DPR. The trip signal shown in Figure 7 which has a minimum time delay is appearing almost the same in all simulations done for different network models if the BW allocation is sufficient. Also, the simulation results showed that the DPR's performance (Integrator value and Tripping time) will be almost unchanged as long as a sufficient BW is allocated regardless of communication network model type that was being used. This performance is shown in Figure 7.

From inspecting Figure 7, it can be clearly seen that even with allocation of a sufficient BW, there is a very small value of time delay (about 10 milliseconds) which may be ignored in many protection applications. Allocating 100% BW to the DPR that is performing estimation can assure that the tripping time delay value is a minimum but in practice, this might not be appropriate because BW that is aggregated/available has to be shared. Also, it can be noted from the inspection of Figure 7 that integrator output will be reset to zero if the current become less than pickup current (78.5 A).

During the transient period that follows the moment of the fault occurrence, both of synchronous machine excitation system and diesel speed governor will react to keep the value of the synchronous speed constant. Graphs in Figure 8 depict the transient stability performance when the communication between the phasor estimation function and the IDMT over-current relay function is accomplished through the different types of the real-time networks at a sufficient BW allocation. As shown in this figure, all graphs have the same performance and the system needs about 2.5 *sec* to recover the stability. The following sub-section illustrates the impact of assigning an insufficient BW on the relay tripping time value that is given in sub-section-2.2 and consequently, how it may affect the transient stability of the selected test power system.

Evaluating the Impact of Bandwidth

To evaluate the impact of BW allocation on DPR tripping time for all types of communication networks being used, the network traffic is made adjustable and

ranges between 10 to 100 in a step of 10 Kilobytes per second. The accuracy of the Kaman filtering estimation function is depending on that there is no loss of samples and those received samples should be available at every time frame for calculation (i.e., no time delay). When the operation of the DPR depends on the Kalman filtering algorithm for estimating the fundamental amplitude, any allocation of BW that is insufficient to handle the traffic burden of samples (i.e., 80 samples/cycle) can cause a delay in the received samples and as a result, unnecessary shift to the relay's integrator graph will occur. Figure 9 shows the performance of DPR when the communication is accomplished based on CSMA AMP, CSMA CD, FDMA, Switched Ethernet and TDMA real-time networks whereas Figure 10 shows the performance based on NCM and ROUND ROBE network types.

When an insufficient BW of 10 Kilobytes per second is allocated, some network types such as CSMA AMP, CSMA CD, FDMA, Switched Ethernet and TDMA have a time delay that made the integrator start grow after a delay of ≈ 1.5 *sec* whereas for NCM and ROUND ROBE networks delay it was ≈ 3.5 *sec*. Graphs in Figure 11 and Figure 12 depict the transient stability performance when the communication between the phasor estimation function and the IDMT over-current relay function is accomplished through the different types of the real-time networks and when an insufficient BW is allocated. When the allocation of BW is increased, the tripping time error decreases until it has a minimum value of almost ≈ 10 milliseconds at an allocation of 80 Kilobytes per second BW or more (fulfilled for all network model types) as shown in Figure 13 in which the bars represent the actual relay time (i.e., nominal operating time of the relay plus time delay error). The value of relay operating time is varying from minimum value of 0.06 *sec* (nominal value= 0.05 *sec* plus error of ≈ 10 milliseconds) for all network models to a maximum value of 1.55 *sec* (nominal value= 0.05 *sec* plus error of ≈ 1.5 *sec*) when communication is accomplished based on CSMA AMP, CSMA CD, FDMA, Switched Ethernet and TDMA models or a maximum value of 3.55 *sec* (nominal value= 0.05 *sec* plus error of ≈ 3.5 *sec*) when communication is accomplished based on NCM and ROUND ROBE network models.

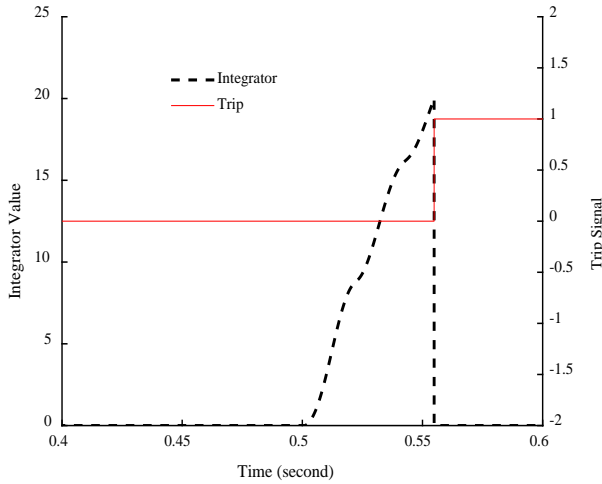


Figure 7. Integrator and Trip signals at sufficient allocation of BW (All network model types)

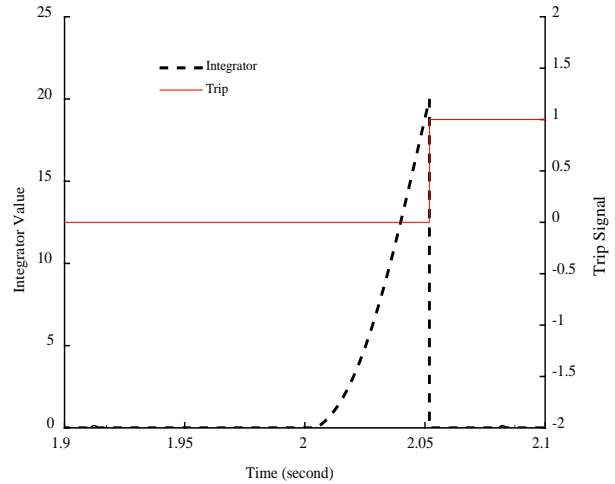


Figure 9. Integrator and Trip signals at sufficient allocation of BW (CSMA AMP, CSMA CD, FDMA, Switched Ethernet and TDMA types).

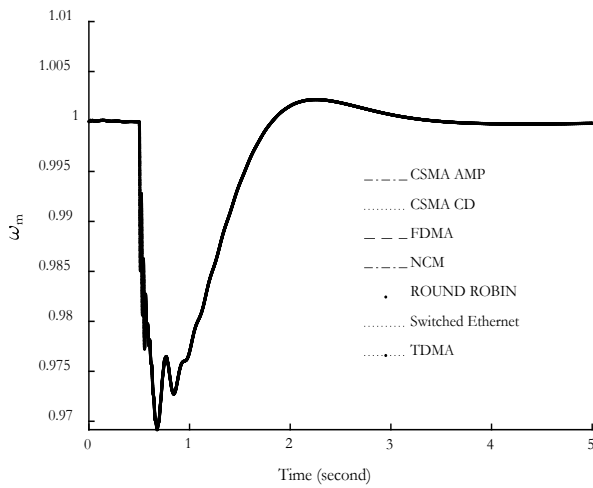


Figure 8. Impact of network model type on transient stability at sufficient BW allocation (All network model types).

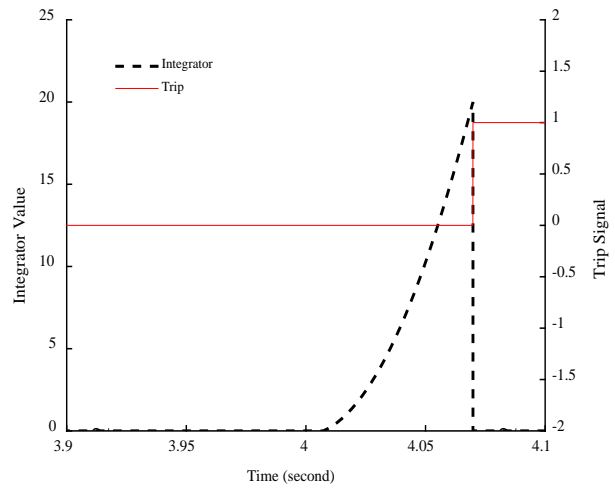


Figure 10. Integrator and Trip signals at sufficient allocation of BW (NCM and ROUND ROBIN network types).

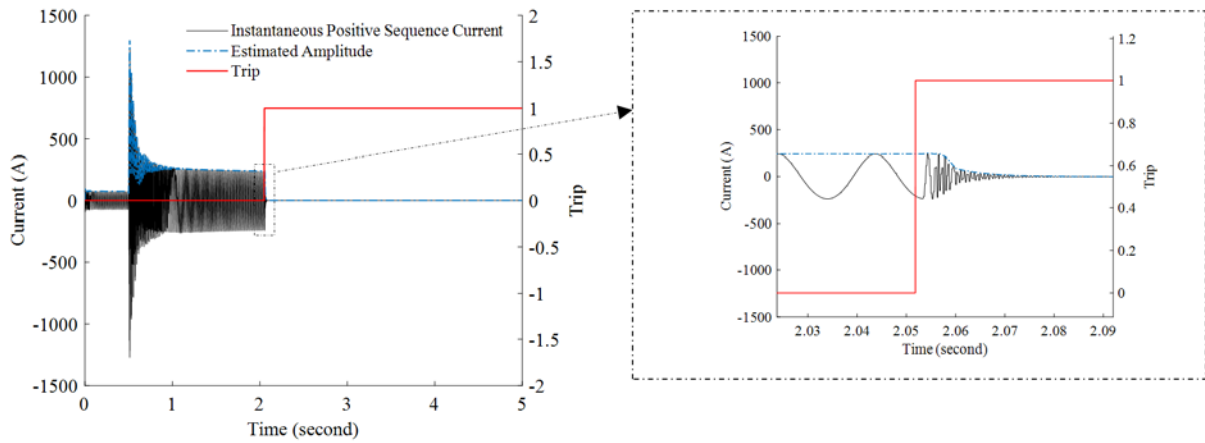


Figure 11. Impact of network model type on transient stability at insufficient BW allocation (CSMA AMP, CSMA CD, FDMA, Switched Ethernet and TDMA types).

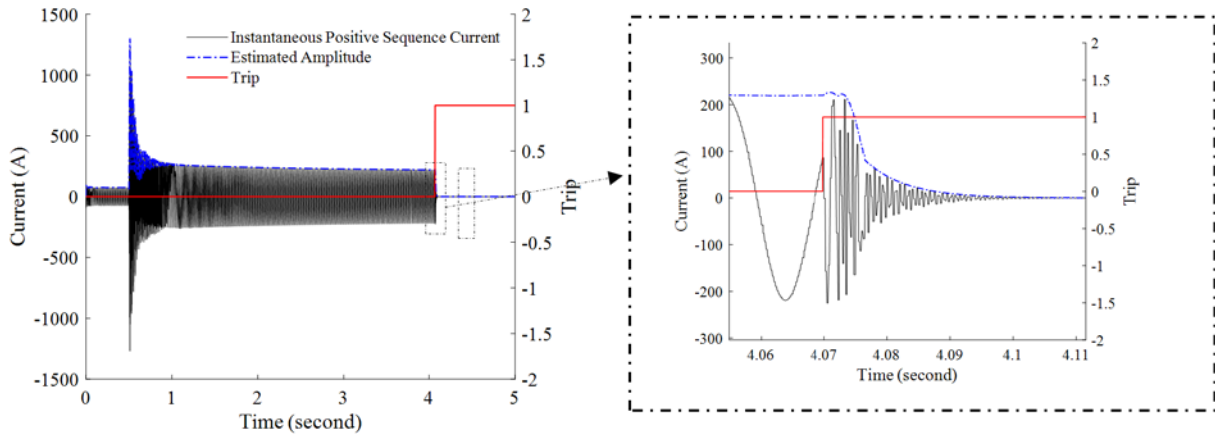


Figure 12. Impact of network model type on transient stability at insufficient BW allocation (NCM and ROUND ROBIN network types).

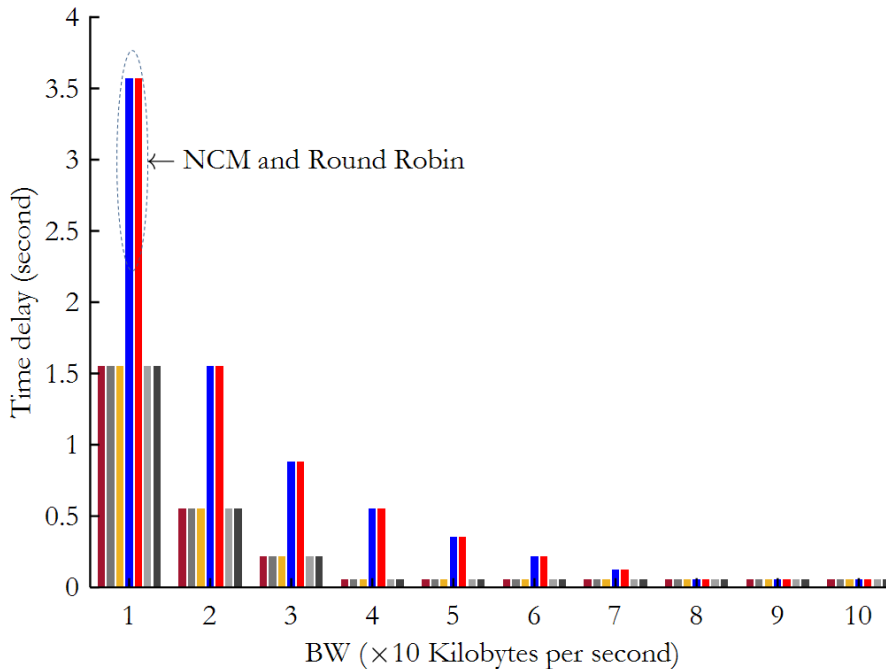


Figure 13. Change in Relay tripping time against BW allocation.

Also, it can be noted from Figure 13 that signals may be classified into two groups: first group, which has same fitted signal with a time delay of 1.5 sec (signals of CSMA AMP, CSMA CD, FDMA, Switched Ethernet, TDMA networks), and second group which has same fitted signal with a time delay of 3.5 sec (signals of NCM and ROUND ROBIN networks).

This classification can help to find another way to estimate the time delay errors by comparing the signal with two reference fitted curves that are representing the signals of first and second groups, respectively. This can easily be done by fitting them to the curve data that is resulted when allocating sufficient BW (as shown in Figure 6) and then, calculating the square root of the variance of the residuals (RMSE). Figure 14 shows how the value of the RMSE is changing against the change of BW allocation. The RMSE value falls to a very small value at 40 Kilobytes per second

BW allocation for CSMA AMP, CSMA CD, FDMA, Switched Ethernet and TDMA networks, whereas it falls to smaller value at 80 Kilobytes per second BW allocation for NCM and ROUND ROBIN networks. Figure 15 shows how the performance of the transient stability can change with the two main categories of signals. It can be observed from the figure that the performance is different from the one shown in Figure 8. In Figure 8, the performance curves are recovered without any drops, whereas in Figure 15 curves have lower drops at the tripping moments and they are eventually recovered. The drops of the curves that are representing the performance of networks of group#1 have maximum peak errors of 0.3% whereas it is 0.16% for group#2. Even though the maximum peak error of curves of group#1 is higher, they are recovered faster than curves of group#2.

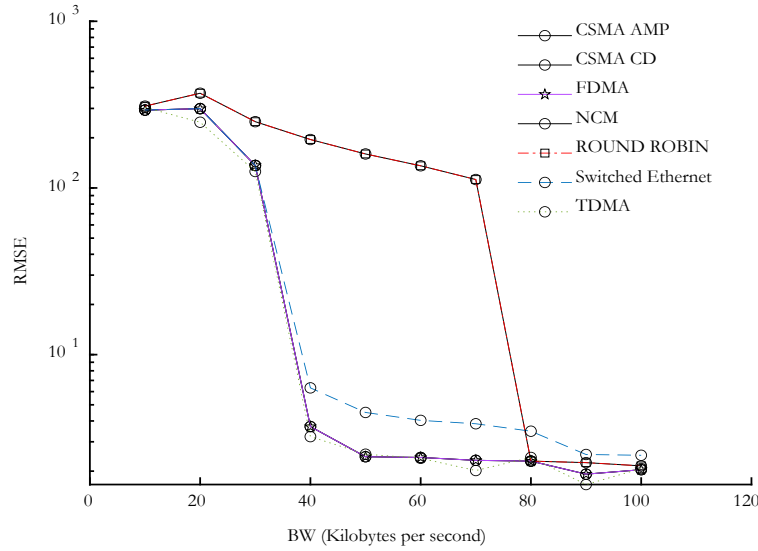


Figure 14. Impact of BW allocation on RMSE.

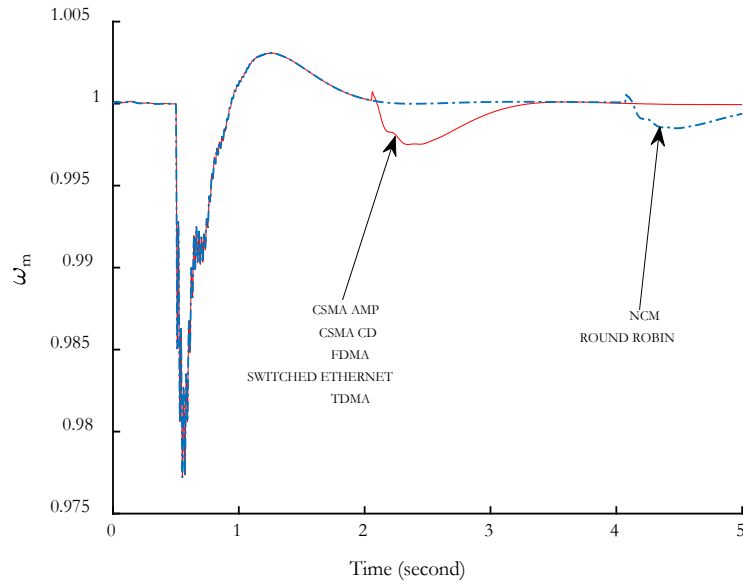


Figure 15. Impact of network model type on transient stability at insufficient BW allocation (All network model types).

Evaluating the Impact of Noise

To evaluate the impact of noise, the communications network was routed through a noise generator block in which an adjustable level of noise can be injected into the network. Also, the BW is allocated at 100% (100 Kilobytes per second) so only the noise can affect the relay performance. The effect of change in covariance (R) of driving noise on the integrator for networks of group#1 (CSMA AMP, CSMA CD, FDMA, Switched Ethernet and TDMA) is shown in Figure 16. As shown, the increase in R has made the curve to shift rightward and more time is needed to reach the pre-determined value of the integrator

which is an indication of time delay.

The tripping time of the relay is increased from 0.055 sec (the delay= 0.055-0.05 sec) when R= 0 to a value of 0.077 sec (the delay= 0.077-0.05 sec) at R= 0.02, so only 27 milliseconds maximum time delay is raised. The maximum value of the tripping time (77 milliseconds or 3.85 cycles) is not more than the 12 cycles condition that is given by Eq. (19) which indicates that the relay will be operational even in presence of an excessive noise. Figure 17 shows the tripping time of relay versus R for all network’s types being used.

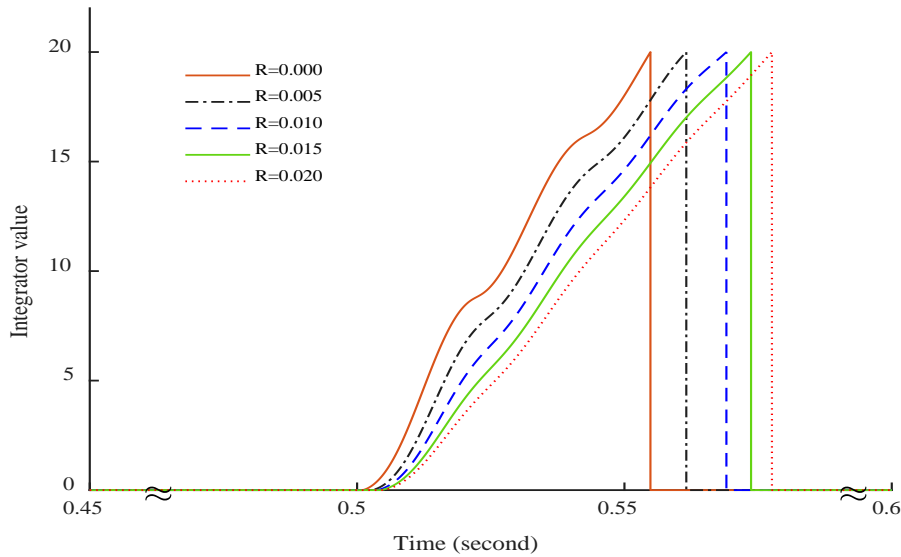


Figure 16. Integrator values vs. time for different values of noise (Only for CSMA AMP, CSMA CD, FDMA, Switched Ethernet and TDMA types)

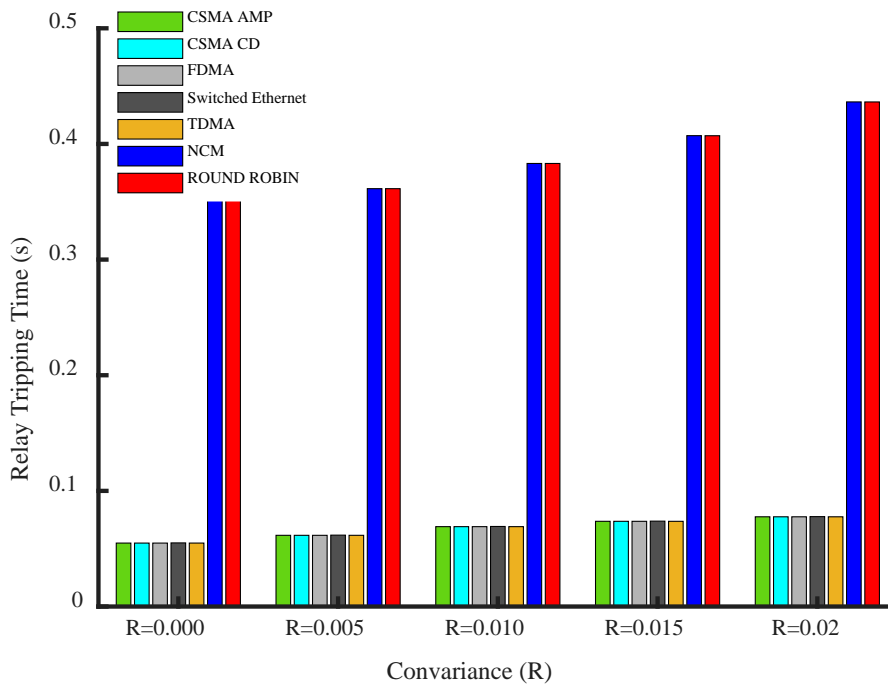


Figure 17. Impact of noise on tripping time.

It is clear from the bars in this figure that when communications are accomplished based on networks belonging to group#2 (NCM and ROUND ROBIN network types), the R becomes more effectively and it can cause a very high tripping delay compared to networks belong to group#1. Actually, this tripping time can reach a value of 0.03863 sec (the delay= 0.3863-0.05 sec), whereas it was just 0.077 sec for group#1 at the same value of noise (R= 0.02). This is an indication of how a slight increase in R can cause malfunction and the relay may fail to trip within the pre-determined time when the communications are accomplished based on networks

belonging to group#2.

5. Conclusions

A new implementation of a scheme that is able to detect any delays in tripping time that may arise in Ethernet-based relays due to insufficient BW allocation or noise is presented in this paper. The results are demonstrated that allocation of insufficient BW can affect the tripping time of DPRs. When the communication is accomplished based on NCM or ROUND ROBIN networks, any insufficient BW

allocation can affect the relay tripping time and the effect is more dramatic than other based networks. The results revealed that at a low value of 10 Kilobytes per second BW allocation, the time delay will be 3.5 sec for NCM and ROUND ROBIN networks and 1.5 sec for the other types of network models. Moreover, results show-ed that the oscillations in rotor speed are increased with the decrease of BW allocations, while it is almost damped when a sufficient BW is allocated. For the noise effect, it has less impact on relay tripping time than BW, whereas the maximum delay record was 336.3 milliseconds recorded. These delay errors must be considered so; a better Ethernet-based network relay setting can be recommended. For future work, the OCR can be replaced with a directional over-current relay thus, the effect of time delay can be evaluated for the maximum sensitivity based on the estimation of the directional phasor angle.

REFERENCES

- [1] A. Abdelmoumene and H. Bentarzi, "A review on protective relays' developments and trends," *Journal of Energy in Southern Africa*, vol. 25, pp. 91-95, 2014.
- [2] N. K. Rajalwal and D. Ghosh, "Recent trends in integrity protection of power system: A literature review," *International Transactions on Electrical Energy Systems*, vol. 30, p. e12523, 2020.
- [3] A. El-Mahdy and M. Seraj-Eldin, "Design of multi-antenna relaying for OFDM in impulsive noise environment," *Digital Communications and Networks*, vol. 5, pp. 189-195, 2019.
- [4] H. Hajizadeh, S.-A. Ahmadi, and M. Sanaye-Pasand, "An Analytical Fast Decaying DC Mitigation Method for Digital Relaying Applications," *IEEE Transactions on Power Delivery*, 2020.
- [5] G. K. Rao, T. Gangwar, and S. Sarangi, "Advanced Relaying for DG-Penetrated Distribution System," *Arabian Journal for Science and Engineering*, pp. 1-13, 2021.
- [6] M. Tajdinian, H. Samet, A. Hamed, A. Hadaeghi, A. Bagheri, M. Allahbakhshi, et al., "Enhancing Immunity of Full-Cycle Discrete Fourier Transform Against Decaying DC Components: a Comparative Analysis," in *2019 IEEE International Conference on Environment and Electrical Engineering and 2019 IEEE Industrial and Commercial Power Systems Europe (EEEIC/I&CPS Europe)*, 2019, pp. 1-6.
- [7] G. Wang, M.-s. Ding, X.-h. Li, and L. Xiao, "Reliability analysis of digital protection," *PROCEEDINGS-CHINESE SOCIETY OF ELECTRICAL ENGINEERING.*, vol. 24, pp. 47-52, 2004.
- [8] S. Xia, X. Chen, and H. Yin, "DFT Based Compression Algorithm for Configuration Coefficients of Reconfigurable Intelligent Surface," in *2021 13th International Conference on Wireless Communications and Signal Processing (WCSP)*, 2021, pp. 1-5.
- [9] X. Wang, T. Jin, L. Hu, and Z. Qian, "Energy-efficient power allocation and Q-learning-based relay selection for relay-aided D2D communication," *IEEE Transactions on Vehicular Technology*, vol. 69, pp. 6452-6462, 2020.
- [10] B. W. Jaekel, "Description and classification of electromagnetic environments-revision of IEC 61000-2-5," in *2008 IEEE International Symposium on Electromagnetic Compatibility*, 2008, pp. 1-4.
- [11] J. Valenzuela and J. Pontt, "Real-time interharmonics detection and measurement based on FFT algorithm," in *2009 Applied Electronics*, 2009, pp. 259-264.
- [12] E. Santos, M. Khosravy, M. A. Lima, A. S. Cerqueira, and C. A. Duque, "ESPRIT associated with filter bank for power-line harmonics, sub-harmonics and inter-harmonics parameters estimation," *International Journal of Electrical Power & Energy Systems*, vol. 118, p. 105731, 2020.
- [13] H.-C. Lin, "Measurement of harmonics and interharmonics using FFT-based algorithm," in *2017 IEEE International Conference on Mechatronics and Automation (ICMA)*, 2017, pp. 1650-1654.
- [14] T. Su, M. Yang, T. Jin, and R. C. C. Flesch, "Power harmonic and interharmonic detection method in renewable power based on Nuttall double-window all-phase FFT algorithm," *IET Renewable Power Generation*, vol. 12, pp. 953-961, 2018.
- [15] M. M. Aman, M. Q. A. Khan, and S. A. Qazi, "Digital directional and non-directional over current relays: Modelling and performance analysis," *NED University Journal of Research*, vol. 8, 2011.
- [16] S. Lv, J. Pan, J. Li, and X. Guo, "Combining Mathematical Morphology and Unscented Kalman Filter for Digital Protective Relaying," *DEStech Transactions on Environment, Energy and Earth Sciences*, 2018.
- [17] J. Zhao and L. Mili, "A decentralized H-infinity unscented Kalman filter for dynamic state estimation against uncertainties," *IEEE Transactions on Smart Grid*, vol. 10, pp. 4870-4880, 2018.
- [18] S. K. Gunda and V. S. S. S. S. Dhanikonda, "Discrimination of Transformer Inrush Currents and Internal Fault Currents Using Extended Kalman Filter Algorithm (EKF)," *Energies*, vol. 14, p. 6020, 2021.
- [19] F. Naseri, Z. Kazemi, E. Farjah, and T. Ghanbari, "Fast detection and compensation of current transformer saturation using extended Kalman filter," *IEEE Transactions on Power Delivery*, vol. 34, pp. 1087-1097, 2019.
- [20] F. Naseri, Z. Kazemi, M. M. Arefi, and E. Farjah, "Fast discrimination of transformer magnetizing current from internal faults: An extended Kalman filter-based approach," *IEEE Transactions on Power Delivery*, vol. 33, pp. 110-118, 2017.
- [21] M. A. Shoaib, A. Q. Khan, G. Mustafa, S. T. Gul, O. Khan, and A. S. Khan, "A framework for observer-based robust fault detection in nonlinear systems with application to synchronous generators in power systems," *IEEE Transactions on Power Systems*, 2021.
- [22] S. Samantaray and P. Dash, "High impedance fault detection in distribution feeders using extended kalman

- filter and support vector machine," *European Transactions on Electrical Power*, vol. 20, pp. 382-393, 2010.
- [23] Y. Yerra, D. Ram Kumar Reddy, and P. Sudheesh, "An Unscented Kalman Filter Approach for High-Precision Indoor Localization," in *Intelligent Manufacturing and Energy Sustainability*, ed: Springer, 2021, pp. 433-441.
- [24] K. K. Challa and G. Gurralla, "Dynamic state and parameter estimation of synchronous generator from digital relay records," *Electric Power Systems Research*, vol. 189, p. 106743, 2020.
- [25] T. Sidhu, E. Demeter, and S. Faried, "A digital relay algorithm for Ethernet-based data transfer," in 2003 IEEE PES Transmission and Distribution Conference and Exposition (IEEE Cat. No. 03CH37495), 2003, pp. 290-295.
- [26] A. Aichhorn, R. Mayrhofer, H. Krammer, and T. Kern, "Realization of line current differential protection over IP-based networks using IEEE 1588 for synchronous sampling," 2016.
- [27] S. M. Blair, C. D. Booth, B. De Valck, D. Verhulst, and K.-Y. Wong, "Modeling and analysis of asymmetrical latency in packet-based networks for current differential protection application," *IEEE Transactions on Power Delivery*, vol. 33, pp. 1185-1193, 2017.
- [28] A. Abdolkhalig and R. Zivanovic, "Simulation and testing of the over-current protection system based on IEC 61850 Process-Buses and dynamic estimator," *Sustainable Energy, Grids and Networks*, vol. 2, pp. 41-50, 2015.
- [29] IEC, "IEC 60255 Standard for Electrical Relays," ed: The International Electrotechnical Commission, 1989.
- [30] Z. Kurt-Yavuz and S. Yavuz, "A comparison of EKF, UKF, FastSLAM2. 0, and UKF-based FastSLAM algorithms," in 2012 IEEE 16th International Conference on Intelligent Engineering Systems (INES), 2012, pp. 37-43.
- [31] D. Hong-de, D. Shao-wu, C. Yuan-cai, and W. Guang-bin, "Performance comparison of EKF/UKF/CKF for the tracking of ballistic target," *TELKOMNIKA Indonesian Journal of Electrical Engineering*, vol. 10, pp. 1692-1699, 2012.
- [32] H. He, H. Qin, X. Sun, and Y. Shui, "Comparison study on the battery SoC estimation with EKF and UKF algorithms," *Energies*, vol. 6, pp. 5088-5100, 2013.
- [33] S. Konatowski, P. Kaniewski, and J. Matuszewski, "Comparison of estimation accuracy of EKF, UKF and PF filters," *Annual of Navigation*, 2016.
- [34] A. Giannitrapani, N. Ceccarelli, F. Scortecchi, and A. Garulli, "Comparison of EKF and UKF for spacecraft localization via angle measurements," *IEEE Transactions on aerospace and electronic systems*, vol. 47, pp. 75-84, 2011.
- [35] U. I. U. Group, "Implementation Guideline for Digital Interface to Instrument Transformers Using IEC 61850 9-2," Second Edition ed: IEC, 2003.
- [36] W. Dueterhoeft, M. W. Schulz, and E. Clarke, "Determination of instantaneous currents and voltages by means of alpha, beta, and zero components," *American Institute of Electrical Engineers, Transactions of the*, vol. 70, pp. 1248-1255, 1951.
- [37] D. Henriksson, A. Cervin, and K.-E. Årzén, "TrueTime: Real-time control system simulation with MATLAB/Simulink," in *Proceedings of the Nordic MATLAB Conference*, 2003.